

Separating Subsurface Scattering from Photometric Images*

Tai-Pang Wu and Chi-Keung Tang
Vision and Graphics Group
The Hong Kong University of Science and Technology
Clear Water Bay, Hong Kong
{pang|cktang}@cs.ust.hk

Abstract

While subsurface scattering is common in many real objects, almost all separation algorithms focus on extracting specular and diffuse components from real images. In this paper, we present a model-less approach derived from the bi-directional surface scattering reflectance distribution function (BSSRDF). In our approach, we show that an illumination image is composed by the Lambertian diffuse and subsurface scattering images. By converting the separation problem into one of two-layer separation in the illumination domain, a Bayesian framework is used to solve the optimization problem which incorporates spatial and illumination constraints, the latter of which are captured as a set of diffuse priors. We present the detailed mathematical formulation and experimental results.

1. Introduction

Subsurface scattering is a complex physical phenomenon, where the outgoing radiance observed at a surface point may be due to the incoming irradiance at *different* surface points. To describe the effect of subsurface scattering, the bi-directional surface scattering reflectance distribution function (BSSRDF) is used [4]. However, BSSRDF is very difficult to capture without the knowledge of object geometry and material property.

Model-based approach Inspired by [7], in [11], a model-based approach was proposed. The mathematical model was derived from the BSSRDF [4] and Lafortune model [5]. This model-based method is capable of handling non-directional subsurface scattering. Using their image acquisition system, contribution due to directional subsurface scattering can be captured together with that of non-directional subsurface scattering. Given a set of images only, the input is decomposed into three photometric components: *off-specular* I_s , non-Lambertian or *local diffuse* D , and *subsurface scattering* I_{scat} . The BSSRDF can describe I_s , D and I_{scat} , but the traditional BRDF can only

describe the local I_s and D . This approach avoids the difficult problem of capturing/recovering the BSSRDF. Because a reflectance model is assumed, it is possible to relight the scene after the optimal model parameters are estimated provided that directional subsurface scattering is negligible.

Model-less approach In this paper, we present a model-less approach that separates subsurface scattering into an aggregate term. However, this approach assumes the absence of specular reflection. Given a single image I only, we decompose the input into two photometric components: *local diffuse* I_{diff} and *subsurface scattering* I_{scat} . This approach uses Bayesian framework to perform optimal separation and estimates the two components from an intrinsic illumination image. Since no model parameters are estimated, no relighting is possible. Our acquisition system captures a set of diffuse priors and is easier to build. Therefore, if the object/scene does not have too much specular reflection and relighting is unnecessary, the model-less method is recommended for reflectance separation.

Our model-less approach is inspired by two-layer separation [2, 8]. By using multiple images, [3] and [9] used motion difference between the reflected and non-reflected layers for their separation. In [6], sparsity priors are used together with user assistance to separate two layers from a single image. By using an intrinsic image, we show in this paper that when the optimization constraints and priors (to be detailed) are available, the reflectance separation problem can be solved to some extent with as few as a single image. Table 1 previews and compares the two approaches. Under different situations, practitioners can choose either method for reflectance separation. The two approaches differ in terms of input, capturing requirement and output.

2. Image Representation

An image I can be represented by a product of two intrinsic images [1], reflectance image ρ and illumination image H . The ρ captures the texture or the shading information while the H captures the illumination distribution over the image. In other words, H can be regarded as a measurement of the scene radiance. If shadow and specular highlight do not exist, H is a composite of $\mathbf{N} \cdot \mathbf{L}$ and \mathcal{A} , where \mathbf{N} is surface normal, \mathbf{L} is lighting direction and intensity

*This research was supported by the Research Grant Council, Hong Kong under grant nos 620005.

	Model-based [11]	Model-less (this paper)
Use of reflectance model	Yes	No
Subsurface scattering	Non-directional modeled, any types captured	any types
Input	six images and three video sequences	one intrinsic image with a set of sampled diffuse priors
Other reflectances considered	off-specular and non-Lambertian diffuse	Lambertian diffuse only
Optimization	model parameters estimation by Levenberg-Marquardt method	diffuse and subsurface scattering components estimation by Bayesian optimization
Relighting	Yes, if only non-directional subsurface scattering is present.	No
Easiness to capture	careful (a new image acquisition system is needed in order to capture model parameters I_{scat} for all pixels)	easy (a sparse set of diffuse priors is readily sampled for \mathcal{D})
Surface geometry	not required	not required

Table 1. Comparison of model-based and model-less approaches

and \mathcal{A} is an ambient term. Mathematically, it is defined as:

$$\begin{aligned} I(x) &= \rho(x)H(x) \\ &= \rho(x)[\mathbf{N}(x) \cdot \mathbf{L}(x) + \mathcal{A}(x)] \end{aligned} \quad (1)$$

When the object material exhibits subsurface scattering property, the $\mathbf{L}(x)$ in the above equation encapsulates the contribution of both diffuse and subsurface scattering components. In the following, we will investigate the form of \mathbf{L} if subsurface scattering is present, so that we can perform reflectance separation in its presence.

The BSSRDF S is defined by:

$$dL(\vec{v}_o, \vec{\omega}_o) = S(\vec{v}_i, \vec{\omega}_i; \vec{v}_o, \vec{\omega}_o) d\Phi_i(\vec{v}_i, \vec{\omega}_i)$$

where $L(\vec{v}_o, \vec{\omega}_o)$ is the outgoing radiance at point \vec{v}_o in direction $\vec{\omega}_o$, $\Phi_i(\vec{v}_i, \vec{\omega}_i)$ is the incident flux at the point \vec{v}_i from direction $\vec{\omega}_i$. By integrating the incident irradiance over all incoming directions and area A on the object surface, the total outgoing radiance at \vec{v}_o is defined as:

$$L_o(\vec{v}_o, \vec{\omega}_o) = \int_A \int_{2\pi} S(\vec{v}_i, \vec{\omega}_i; \vec{v}_o, \vec{\omega}_o) L_i(\vec{v}_i, \vec{\omega}_i) (\vec{n}_i \cdot \vec{\omega}_i) d\vec{\omega}_i dA$$

Since we adopt an appearance-based approach, the above equation is rewritten into a discrete form:

$$energy(x_0) = energy(\vec{v}_0) \quad (2)$$

$$= \sum_{i=0}^n S(\vec{v}_i, \mathbf{L}(\vec{v}_i); v_0, \mathbf{L}(v_0)) \mathbf{N}(\vec{v}_i) \cdot \mathbf{L}(\vec{v}_i) \quad (3)$$

Note that $energy(x_0)$ is the outgoing radiance measured at x_0 , which is an image of of \vec{v}_0 . By rotating the local coordinate system of each surface patch at \vec{v}_i with rotation matrix ψ_i such that $\mathbf{N}(\vec{v}_i)$ aligns with $\mathbf{N}(\vec{v}_0)$, the above

equation becomes:

$$energy(x_0) = \mathbf{N}(x_0) \cdot \left[\sum_{i=0}^n S(x_i, \mathbf{L}(x_i); x_0, \mathbf{L}(x_0)) (\psi_i \mathbf{L}(x_i)) \right] \quad (4)$$

where x_i is the image point of \vec{v}_i , and \mathbf{L} and \mathbf{N} are overloaded functions that return the light direction and normal at x and v respectively. From this equation, it can be observed that the original $\mathbf{L}(x_0)$ is resized by $S(x_0, \mathbf{L}(x_0); x_0, \mathbf{L}(x_0))$ and jittered due to the contribution of the energy from other points \vec{v}_i . By rewriting the above equation, we have:

$$energy(x_0) = \mathbf{N}(x_0) \cdot [\beta(x_0)\mathbf{L}(x_0) + \mathbf{L}_{scat}(x_0)] \quad (5)$$

where $\beta(x_0) = S(x_0, \mathbf{L}(x_0); x_0, \mathbf{L}(x_0))$ and $\mathbf{L}_{scat}(x_0) = \sum_{i=1}^n S(\vec{v}_i, \mathbf{L}(\vec{v}_i); x_0, \mathbf{L}(x_0)) (\psi_i \mathbf{L}(\vec{v}_i))$. Note that $\beta(x_0)$ does not depend on other image points.

Suppose the ambient term is not significant. H in Eqn (1) measures the outgoing energy, so by setting $x = x_0$ in Eqn (5) and putting it into Eqn (1), we have:

$$I(x) = \rho(x)\mathbf{N}(x) \cdot [\beta(x)\mathbf{L}(x) + \mathbf{L}_{scat}(x)] \quad (6)$$

$$= \rho(x)(H_{diff}(x) + H_{scat}(x)) \quad (7)$$

where $H_{diff}(x) = \beta(x)\mathbf{N}(x) \cdot \mathbf{L}(x)$ and $H_{scat}(x) = \mathbf{N}(x) \cdot \mathbf{L}_{scat}(x)$. From the mathematical definition, it can be seen that $H_{diff}(x)$ and $H_{scat}(x)$ are the *diffuse illumination image* and the *subsurface scattering illumination image* respectively. Moreover, H_{scat} captures any types of subsurface scattering contribution, since S in Eqn (3) is of the most general form.

Using the image representation, the remaining problem is how to separate ρ , H_{diff} and H_{scat} from the illumination image I . Since reflectance separation is an inverse process of image formation, we only know I . The goal of our work is to separate the components of diffuse and subsurface scattering. That is, given I , we want to find the diffuse

component $I_{diff} = \rho H_{diff}$ and the subsurface component $I_{scat} = \rho H_{scat}$.

3. Constraints

To simplify the problem, some unknowns should be estimated first. One choice is to estimate ρ first. By Eqn (7), we found that subsurface scattering only modifies the illumination image H . It implies that some existing intrinsic image separation methods which deal with Eqn (1) can be used to find ρ and, consequently, H .

Suppose ρ and H are known. If we can separate H_{diff} and H_{scat} from H , equivalently, we can find I_{diff} and I_{scat} . So, in the following, we focus on how to find H_{diff} and H_{scat} . In fact, we only need to find H_{diff} because $H_{scat} = H - H_{diff}$.

Since H is just the addition of two images, we consider the reflectance separation problem as a two-layer image separation problem. However, given H only, there is a large number of possibilities of H_{diff} and H_{scat} . This implies that constraints have to be applied in order to obtain a reasonable estimation.

Spatial constraint analysis One of the important observations is that the appearance of H , H_{diff} and H_{scat} are very similar because they capture the same object. It implies that the smoothness between a pair of neighboring pixels is very similar in all the three images respectively. The above observation indicates that H has a very similar structure to H_{diff} as well as H_{scat} . This implies that if $(H(x) - H(y))^2$ is small, $(H_{diff}(x) - H_{diff}(y))^2$ is small and vice versa, where x and y are neighboring pixels.

Illumination constraint analysis The constraint described above only considers the structure of objects, or image smoothness. By using the above constraint alone is inadequate to perform separation because we want not only to maintain the structure, but also to redistribute the illumination contribution appropriately to the two images, H_{diff} and H_{scat} . To do so, we at least need to know some of the pixels in H_{diff} . We call these pixels *diffuse priors*. However, I , ρ and H do not provide such information. This implies that extra work is needed to obtain the required priors.

Consider a *single* light ray incident on the surface of an object. Except at the point of incidence, the outgoing radiance from other points of the object surface is entirely due to subsurface scattering. As described in the previous subsection, S is bell-shaped with the peak located at the point of incidence. Thus, after image formation, the pixel location with the peak response gives the following important information: 1) the image of the point of incidence, and 2) only Lambertian diffuse reflection occurs at that pixel. So, if such an image exists, we can search through the image to find the peak at which Lambertian diffuse reflection occurs. By collecting a set of such images, we obtain some illumination constraints to estimate the diffuse component.

4. Bayesian Optimization

Considering the above two constraints, we solve the separation problem by applying the Bayesian framework. Define $\mathcal{D} = \{\kappa(y)|y \in W\}$ to be a set of known diffuse priors, where W is a set of pixel locations at which known peak responses occur, and $\kappa(y)$ is the intensity at pixel y . We maximize the *a posteriori probability* (MAP) to infer H_{diff}^* , given the observation from H and \mathcal{D} :

$$H_{diff}^* = \arg \max_{H_{diff}} p(H_{diff}|H, \mathcal{D}) \quad (8)$$

$$= \arg \max_{H_{diff}} p(H, \mathcal{D}|H_{diff})p(H_{diff}) \quad (9)$$

Since we do not have any prior information from H_{diff} , $p(H_{diff})$ is considered as a uniform distribution and is ignored in the above equation. Next, we define the likelihood $p(H, \mathcal{D}|H_{diff})$.

Likelihood The likelihood in Eqn (9) can be factorized under the i.i.d. assumption:

$$p(H, \mathcal{D}|H_{diff}) = p(H|H_{diff})p(\mathcal{D}|H_{diff}) \quad (10)$$

$$= p(H|H_{diff}) \prod_{y \in W} p(\kappa(y)|H_{diff}) \quad (11)$$

The smoothness of H should be maintained in H_{diff} . So, we can use the illumination difference of all pairs of neighboring pixels in H as the weight to measure the smoothness of H_{diff} . Define M_x to be the set of neighboring pixels of x and $u \in M_x$. If a pair of neighboring pixel is smooth, $(H(x) - H(u))^2$ is small and $(H_{diff}(x) - H_{diff}(u))^2$ has to be small too. Thus, we can use $1 - (H(x) - H(u))^2$ to weigh the smoothness in H_{diff} . The likelihood $p(H|H_{diff})$ is modeled as:

$$\exp\left(-\frac{\sum_x \sum_{u \in M_x} [1 - (H(x) - H(u))^2]^d [H_{diff}(x) - H_{diff}(u)]^2}{2\sigma_H^2}\right)$$

where d controls the strictness of the weighting and σ_H^2 is the variance term to model the uncertainty.

The illumination constraint has to be maintained in order to redistribute the illumination contribution to H_{diff} and H_{scat} . We have to minimize the image difference between known diffuse component and estimated diffuse component. Thus, $p(\kappa(y)|H_{diff})$ of the likelihood is modeled as follow:

$$p(\kappa(y)|H_{diff}) \propto \exp\left(-\frac{(H_{diff}(y) - \kappa(y))^2}{2\sigma_k^2}\right) \quad (12)$$

where σ_k^2 is a variance to model the uncertainty.

However, $p(\kappa(y)|H_{diff})$ defined as the form of Eqn (12) is not enough. If the illumination constraint at y is completely satisfied while the measured $\kappa(y)$ contains error, the intensity of neighboring pixels of y may have large contrast compared to that of y . This will produce impulse noise at y . To solve this problem, we do not allow sudden change in intensity between y and its neighboring pixels. Thus, we also consider the second derivative at y to minimize the change. Eqn (12) becomes:

$$p(\kappa(y)|H_{diff}) \propto \exp\left(-\frac{(H_{diff}(y) - \kappa(y))^2}{2\sigma_k^2}\right) \quad (13)$$

$$\exp\left(-\frac{(-4H_{diff}(y) + \sum_{u \in G_y} H_{diff}(u))^2}{2\sigma_d^2}\right)$$

where $\sigma_i^2, i = k, d$, are variances to model the uncertainty and G_y denotes the indices of the first-order (upper, lower, left and right) neighbors of y .

MAP Solution With Eqn (9) and the analysis in the previous section, we solve the optimization problem by minimizing the log posterior function:

$$Err(H_{diff}) = -\log p(H|H_{diff}) - \sum_{y \in W} \log p(\kappa(y)|H_{diff}) \quad (14)$$

It can be easily observed that Err is a quadratic objective function. Although there is no local minima, it is difficult to solve the equation by singular value decomposition (SVD) because there are too many variables. We prefer to use an iterative approach to perform the optimization.

5. Experimental Results

We have applied our separation method to a real object, a plastic wine stopper (Fig. 1(a)), which exhibits strong directional subsurface scattering (as shown in Fig. 1(b)). This object possesses some specular effect not considered by our model-less approach, so it also tests the robustness of our method. First, we applied the method in [10] to find the reflectance image (Fig. 1(d)) ρ and the illumination image H (normalized in Fig. 1(e) for illustration), from the single input image. To capture our diffuse priors, we placed the light source at a large distance from the object to approximate directional light source, and used a cardboard with a small hole pierced to produce a single light ray. We call the captured image a PSF image (e.g. Fig. 1(b), normalized for illustration). The separated diffuse $I_{diff} = \rho H_{diff}$ and subsurface scattering $I_{scat} = \rho H_{scat}$ components are shown in Fig. 1(f) and (g) respectively. The I_{diff} result is very reasonable. In particular, note the purely Lambertian diffuse reflection we separated. The shadow region of I_{diff} are completely dark, while the intensity of the corresponding region in the I_{scat} are non-zero due to subsurface scattering. This shows that our approach correctly handles the diffusion of intensity beneath the object surface.

6. Conclusion

Starting from the more general BSSRDF, a Bayesian optimization framework is formulated for reflectance separation in presence of subsurface scattering. In the future, we will study the effect of sampling of diffuse priors, relax the assumption of absence of specular effect in the model-less approach, and apply our theories in appearance-based and image-based modeling.

References

[1] H.G. Barrow and J.M. Tenenbaum. Recovering intrinsic scene characteristics from images. In *A. Hanson and E. Riseman, editors, Computer Vision System. Academic Press*, pages 3–26, 1978.

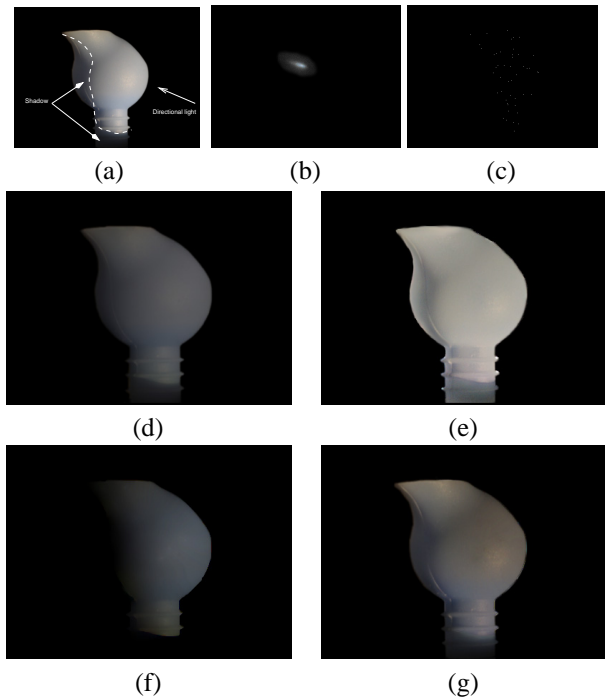


Figure 1. (a) Original input image I . (b) A normalized PSF image for which the peak is sampled as a diffuse prior. Note that the bell-shaped PSF is asymmetric due to the strong contribution of directional subsurface scattering. (c) Distribution of the 47 sampled diffuse priors. (d) Reflectance image of the input image. (e) Normalized illumination image of the input image, (f) Estimated diffuse component I_{diff} , (g) Estimated subsurface scattering component I_{scat} . (See pdf file for more clarity.)

- [2] H. Farid and E.H. Adelson. Separating reflections from images by use of independent components analysis. *16(9):2136–2145*, 1999.
- [3] M. Irani and S. Peleg. Image sequence enhancement using multiple motions analysis. In *CVPR92*, pages 216–221, 1992.
- [4] H. W. Jensen, S. R. Marschner, M. Levoy, and P. Hanrahan. A practical model for subsurface light transport. In *SIGGRAPH01*, pages 511–518, 2001.
- [5] E. P. F. Lafortune, S. Foo, K. E. Torrance, and D. P. Greenberg. Non-linear approximation of reflectance function. In *SIGGRAPH97*, pages 117–126, 1997.
- [6] A. Levin and Y. Weiss. User assisted separation of reflections from a single image using a sparsity prior. In *ECCV04*, volume I, pages 602–613, 2004.
- [7] S. Lin and S. Lee. A representation of specular appearance. In *ICCV99*, pages 849–854, 1999.
- [8] Y. Shechner, J. Shamir, and N. Kiryati. Polarization-based decorrelation of transparent layers: The inclination angle of an invisible surface. In *ICCV99*, pages 814–819, 1999.
- [9] R. Szeliksi, S. Avidan, and P. Anandan. Layer extraction from multiple images containing reflections and transparency. In *CVPR00*, volume 1, pages 246–253, 2000.
- [10] Y. Weiss. Deriving intrinsic images from image sequences. In *ICCV01*, pages 68–75, Jul 2001.
- [11] T.P. Wu and C.K. Tang. Separating specular, diffuse, and subsurface scattering reflectances from photometric images. In *ECCV04*, pages Vol II: 419–433, 2004.